

14. Schulte, S. & Müller, P. J. Variations of sea surface temperature and primary productivity during Heinrich and Dansgaard-Oeschger events in the northeastern Arabian Sea. *Geo-Mar. Lett.* **21**, 168–175 (2001).
15. Hendy, I. L. & Kennett, J. P. Tropical forcing of North Pacific intermediate water distribution during Late Quaternary rapid climate change? *Quat. Sci. Rev.* **22**, 673–689 (2003).
16. Ortiz, J. D. *et al.* Enhanced productivity off western North America during the warm climate intervals of the past 52 k.y. *Geology* **32**, 521–524 (2004).
17. Kiefer, T. *Productivity and Temperatures in the Subtropical North Atlantic: Cyclic and Abrupt Changes During the Late Quaternary* (Rep. No. 90, Geol.-Paläont. Inst. Univ. Kiel, 1998).
18. Lebreiro, S. M., Moreno, J. C., Abrantes, F. F. & Pflaumann, U. Productivity and paleoceanographic implications on the Tore Seamount (Iberian Margin) during the last 225 kyr: Foraminiferal evidence. *Paleoceanography* **12**, 718–727 (1997).
19. Bopp, L. *et al.* Potential impact of climate change on marine export production. *Glob. Biogeochem. Cycles* **15**, 81–100 (2001).
20. Weaver, A. J. *et al.* The UVic Earth system climate model: Model description, climatology and applications to past, present and future climates. *Atmosphere-Ocean* **4**, 361–428 (2001).
21. Simmons, H. L., Jayne, S. R., St Laurent, L. C. & Weaver, A. J. Tidally driven mixing in a numerical model of the ocean general circulation. *Ocean Model.* **6**, 245–263 (2004).
22. Schmittner, A., Oschlies, A., Giraud, X., Eby, M. & Simmons, H. L. A global model of the marine ecosystem for long term simulations: sensitivity to ocean mixing, buoyancy forcing, particle sinking and dissolved organic matter cycling. *Glob. Biogeochem. Cycles* (in the press).
23. Six, K. D. & Maier-Reimer, E. Effects of plankton dynamics on seasonal carbon fluxes in an ocean general circulation model. *Glob. Biogeochem. Cycles* **10**, 559–583 (1996).
24. Schartau, M. & Oschlies, A. Simultaneous data-based optimization of a 1D-ecosystem model at three locations in the North Atlantic: Part I—Method and parameter estimates. *J. Mar. Res.* **61**, 765–793 (2003).
25. Gregg, W. W., Conkright, M. E., Ginoux, P., O'Reilly, J. E. & Casey, N. W. Ocean primary production and climate: Global decadal changes. *Geophys. Res. Lett.* **30**, 1809, doi:10.1029/2003GL016889 (2003).
26. Antoine, D., André, J.-M. & Morel, A. Oceanic primary production 2. Estimation at global scale from satellite (coastal zone color scanner) chlorophyll. *Glob. Biogeochem. Cycles* **10**, 57–69 (1996).
27. Aumont, O., Maier-Reimer, E., Blain, S. & Monfray, P. An ecosystem model of the global ocean including Fe, Si, P colimitations. *Glob. Biogeochem. Cycles* **17**, 1060, doi:10.1029/2001GB001745 (2003).
28. Conkright, M. E. *et al.* *World Ocean Atlas 2001, Objective Analysis, Data Statistics, and Figures* (CD-ROM Documentation, National Oceanographic Data Center, Silver Spring, Maryland, 2002).

Acknowledgements Productivity data sets were provided by D. Antoine and W. Gregg. Discussions with A. Oschlies, M. Sarnthein, M. Weinelt and H. Kinkel were appreciated. This research was supported as part of the research unit (Forschergruppe 451) on ocean gateways by the Deutsche Forschungsgemeinschaft (DFG).

Competing interests statement The authors declare that they have no competing financial interests.

Correspondence and requests for materials should be addressed to A.S. (aschmittner@coas.oregonstate.edu).

Structural and temporal requirements for geomagnetic field reversal deduced from lava flows

Brad S. Singer¹, Kenneth A. Hoffman², Robert S. Coe³, Laurie L. Brown⁴, Brian R. Jicha¹, Malcolm S. Pringle⁵ & Annick Chauvin⁶

¹Department of Geology and Geophysics, University of Wisconsin, Madison, Wisconsin 53706, USA

²Physics Department, California Polytechnic State University, San Luis Obispo, California 93407, USA

³Earth Sciences Department, University of California, Santa Cruz, California 95064, USA

⁴Department of Geosciences, University of Massachusetts, Amherst, Massachusetts 01003, USA

⁵Department of Earth, Atmospheric, and Planetary Sciences, Massachusetts Institute of Technology, Cambridge, Massachusetts 02139, USA

⁶Geosciences Rennes UMR-CNRS, Campus Beaulieu, Bâtiment 15, 35042 Rennes Cedex, France

Reversals of the Earth's magnetic field reflect changes in the geodynamo—flow within the outer core—that generates the field. Constraining core processes or mantle properties that induce or modulate reversals requires knowing the timing and morphology of field changes that precede and accompany these reversals^{1–4}. But the short duration of transitional field states

and fragmentary nature of even the best palaeomagnetic records make it difficult to provide a timeline for the reversal process^{1,5}. ⁴⁰Ar/³⁹Ar dating of lavas on Tahiti, long thought to record the primary part of the most recent 'Matuyama–Brunhes' reversal, gives an age of 795 ± 7 kyr, indistinguishable from that of lavas in Chile and La Palma that record a transition in the Earth's magnetic field, but older than the accepted age for the reversal. Only the 'transitional' lavas on Maui and one from La Palma (dated at 776 ± 2 kyr), agree with the astronomical age for the reversal. Here we propose that the older lavas record the onset of a geodynamo process, which only on occasion would result in polarity change. This initial instability, associated with the first of two decreases in field intensity, began ~18 kyr before the actual polarity switch. These data support the claim⁶ that complete reversals require a significant period for magnetic flux to escape from the solid inner core and sufficiently weaken its stabilizing effect⁷.

Most reversal records come from quasi-continuously deposited sediments^{1,8–9} and many indicate that reversals occur when field intensity has diminished (see, for example, refs 10, 11). Establishing the rate of sediment accumulation may reveal a duration for the reversal process, but accumulation rates are difficult to quantify¹. One approach is to tune oxygen isotope variations orbitally down the section, estimate the astronomical ages of successive magnetic reversals¹² and interpolate the accumulation rate. With the use of

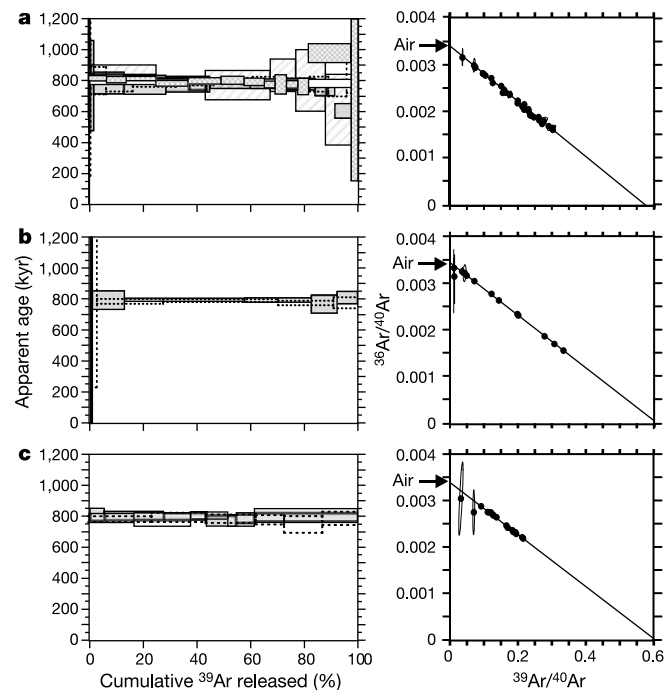


Figure 1 ⁴⁰Ar/³⁹Ar age spectra and isochrons from lavas TT, R1T and R1V in Punaaru Valley, Tahiti. The largely concordant spectra (left) and well-defined isochrons (right) indicate that extraneous argon is not a problem. Isochrons of several experiments on each lava were normalized to a common neutron fluence parameter *J* for illustrative purposes only. The weighted mean of the individual isochrons from several subsamples gives the best age (±2σ) for each lava. **a**, TT groundmass. The plateau is at 789.7 ± 5.2 kyr; the results are from five separate experiments. The isochron age is 798.0 ± 11.0 kyr, ⁴⁰Ar/³⁶Ar_i = 293.9 ± 3.6, MSWD = 0.15 and *n* = 32 of 39. **b**, R1V groundmass. The plateau is at 789.4 ± 6.5 kyr; the results are from two separate experiments. The isochron age is 791.9 ± 9.3 kyr, ⁴⁰Ar/³⁶Ar_i = 294.8 ± 1.9, MSWD = 0.04 and *n* = 13 of 13. **c**, R1T groundmass. The plateau is at 792.1 ± 7.6 kyr; the results are from three separate experiments. The isochron age is 798.0 ± 23.0 kyr, ⁴⁰Ar/³⁶Ar_i = 294.6 ± 2.9, MSWD = 0.70 and *n* = 18 of 18.

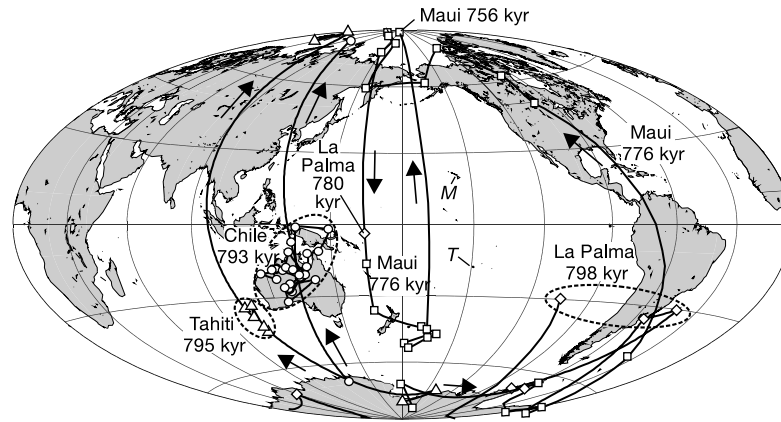


Figure 2 Virtual Geomagnetic Poles (VGPs) and paths of four lava sequences that record transitional directions between 795 and 775 kyr ago. Mean ages of each lava sequence are from Table 1 in thousands of years. The youngest sequence at Maui begins with VGPs in Antarctica that progress through the Americas, sweep clockwise through Alaska

and then move down to a cluster southeast of New Zealand; it is capped by a long series of normally magnetized flows, of which the lowest is dated at 756 kyr ago. M and T indicate the locations of Maui and Tahiti, respectively.

this method on several sediment cores, the average duration of the last four reversals, including the most recent Matuyama–Brunhes (M–B) reversal, is $6,992 \pm 1,089$ yr (2σ)¹³. However, the duration is dependent on the latitude of the observation site, increasing from low latitudes polewards from about 2 to 10 kyr¹³.

Thermoremanent magnetization of lava flows also records reversals; however, each lava in a sequence of flows provides only an instantaneous ‘spot’ recording of the field, so no single sequence is able to capture a reversal in its entirety^{1,4,14}. Notwithstanding this, an advantage is that lavas can be dated precisely using the ⁴⁰Ar/³⁹Ar variant of the K–Ar geochronometer^{15–18}. Our approach to resolving field changes attending a reversal is to examine the palaeomagnetic directions and ⁴⁰Ar/³⁹Ar chronology of four lava sequences that presumably erupted during the M–B reversal.

Three of these sequences met criteria for incorporation into a

global database for the M–B reversal¹⁹: Punaruu Valley, Tahiti^{20,21}; Tataru–San Pedro, Chile^{18,21–22}; and Haleakala, Maui^{17,21}. The fourth sequence on La Palma, Canary Islands, was characterized recently¹⁶. On the basis of the ages of eight lavas from these four sequences, used originally to argue that the duration of the M–B reversal was at least 12 kyr (ref. 21), our goal was to expand the data set and test the hypothesis that the duration of the reversal exceeds the ~7,000-yr average inferred from sediments¹³. We present new ⁴⁰Ar/³⁹Ar ages of transitionally magnetized lavas from Tahiti alongside ages from the other three lava recordings and palaeointensity records from marine sediment, which together illustrate that the change in polarity may be a late stage of the reversal process.

The same ⁴⁰Ar/³⁹Ar incremental heating method^{15–18} and inter-calibrated standard values²³ employed to date 20 transitionally magnetized lavas on Maui, Chile and La Palma were used to date

Table 1 ⁴⁰Ar/³⁹Ar incremental heating ages of transitionally magnetized lavas

Location	Flow unit	Ref.	VGP		No. of experiments			Concordant increments	% of total ³⁹ Ar	Isochron calculation		
			Lat.	Long.	UW	GE	SU			MSWD	⁴⁰ Ar/ ³⁶ Ar _i ± 2σ	Age (kyr) ± 2σ
Haleakala	59	17	-44.2	190.8	3	1	2	50 of 59	94.7	0.96	296.5 ± 1.3	774.2 ± 3.6
	58	17	-47.9	191.3	2	2	1	34 of 45	79.5	1.16	295.7 ± 1.1	778.3 ± 5.2
	52	17	-38.2	163.3				8 of 13	78.0	11.73	293.4 ± 7.2	782.4 ± 26.4
	50	17	75.7	142.8				9 of 14	82.1	0.34	296.8 ± 1.5	778.7 ± 6.9
	45	17	77.5	222.8				9 of 14	85.1	1.38	293.9 ± 0.8	785.1 ± 8.0
	37	17	-67.5	180.9	5		1	47 of 61	87.5	1.30	295.3 ± 0.8	773.0 ± 3.0
<i>Weighted mean age for six lavas from Haleakala</i>												
Chile	QTW11-17	18	-9.8	136.0	3			17 of 18	96.3	0.20	295.4 ± 0.8	801.0 ± 12.0
	QTW11-16	18	-24.8	137.8	2			17 of 22	92.6	1.02	294.2 ± 1.8	791.3 ± 7.9
	QTW11-11	18	-26.1	143.7	1			9 of 13	82.7	1.02	295.5 ± 4.5	792.9 ± 17.1
	QTW11-5	18	-25.7	126.3	3			20 of 24	88.8	1.44	293.6 ± 3.2	793.8 ± 9.8
	QTW11-3	18	-21.8	130.3	2			12 of 23	68.0	0.68	292.6 ± 4.1	795.0 ± 21.0
	QTW10-10	18	-18.9	147.6		1		8 of 11	76.9	0.42	296.7 ± 5.4	790.1 ± 12.6
	QTW10-8	18	-18.7	156.4		3		19 of 26	80.6	0.76	294.4 ± 2.7	790.8 ± 6.7
	QTW10-5	18	-14.4	145.5			2	11 of 13	86.3	1.09	297.5 ± 3.8	790.3 ± 8.6
	QTW10-3	18	-3.4	138.2	2	3		44 of 57	77.5	2.00	292.2 ± 2.8	790.2 ± 6.1
<i>Weighted mean age for nine Chilean lavas</i>												
Tahiti	TT		-34.0	104.6	3	2		32 of 39	83.5	0.15	293.9 ± 3.6	798.0 ± 11.0
	R1V		-33.1	108.6	2			13 of 13	100.0	0.04	294.8 ± 1.9	791.9 ± 9.3
	R1T		-41.9	107.9	3			18 of 18	100.0	0.70	294.6 ± 2.9	798.0 ± 23.0
<i>Weighted mean age for three Tahitian lavas</i>												
La Palma	TN-16	16	-5.4	161.6	5			43 of 59	81.2	1.41	296.3 ± 1.3	780.3 ± 10.3
	TN-17	16	-31.1	250.9	5			34 of 46	82.9	1.40	293.9 ± 1.5	803.3 ± 9.3
	TN-18	16	-70.3	52.0	5			56 of 56	100.0	1.01	294.7 ± 1.7	796.2 ± 10.3
	TN-20b	16	-31.6	313.3	4			39 of 50	91.4	1.81	294.0 ± 2.5	791.2 ± 18.9
	CB202a	21	-48.0	301.0		2		15 of 23	81.0	1.29	299.8 ± 3.8	786.2 ± 27.2
<i>Weighted mean age for four lavas from La Palma</i>												
										0.70		798.4 ± 6.3

All ages are relative to a common 28.34-Myr-old Taylor Creek sanidine standard²³, reported with analytical uncertainty only. Systematic uncertainties in, for example, the ⁴⁰K decay constant, need not be considered when comparing between these ages. Laboratories: UW, Wisconsin; GE, Geneva; SU, Scotland.

three of the five transitional lavas in the Punaruu section. To improve precision, ages and 2σ analytical uncertainties are calculated as the inverse-variance weighted mean obtained from one to six subsamples of each lava^{15–18}. Eight new experiments yielded mainly concordant age spectra, well-defined isochrons of 798.0 ± 23.0 , 791.9 ± 9.3 and 798.0 ± 11.0 kyr, and show no evidence for inherited or excess argon (Fig. 1; see Supplementary Information). The Punaruu sequence describes a reverse–transitional–normal (R–T–N) directional path with clustering of five virtual geomagnetic poles (VGPs) southwest of Australia²⁰ (Fig. 2). The similar VGPs and ages give reason^{15–18} to use the weighted mean of the three isochrons of 794.8 ± 6.8 kyr as the most precise estimate of time since the transitional field was recorded (Table 1).

At La Palma, seven basaltic flows record a R–T–R–T–N sequence of VGPs¹⁶ (Fig. 2). The ages of the three lowermost transitional lavas, with VGPs over southern South America, are indistinguishable from one another and give a weighted mean of 798.4 ± 6.3 kyr that is also not different from that of the three Tahitian lavas (Table 1). The stratigraphically highest transitional lava TN-16 at La Palma yields an age of 780.3 ± 10.3 kyr, which is significantly younger than the mean of the lower three lavas in the section, and younger than the Tahitian lavas (Table 1). Moreover, lava TN-16 has a VGP northeast of Australia that differs from the underlying flows¹⁶ (Fig. 2).

At Tatara-San Pedro volcano 30 andesitic lava flows exhibit R–T–N directions with a tight clustering of VGPs over northern Australia¹⁸ (Fig. 2). Earlier K–Ar²² and $^{40}\text{Ar}/^{39}\text{Ar}$ ages²¹ implied that these lavas record the M–B reversal. Nine of these lavas yield a weighted mean age of 791.7 ± 3.0 kyr (ref. 18) identical to those obtained at La Palma and Tahiti (Table 1).

A section of basaltic lavas at Haleakala volcano includes 24 with VGP latitudes that cluster into three groups, including six between -80° and -45° at the base, seven between $+40^\circ$ and 75° in the middle, followed by eight between -35° and -50° near the top¹⁷ (Fig. 2). $^{40}\text{Ar}/^{39}\text{Ar}$ ages of six flows are indistinguishable from one another and give a weighted mean of 775.6 ± 1.9 kyr (Table 1), indicating that this sequence corresponds to the M–B reversal¹⁷. The mean age of the Maui sequence is significantly younger than that of the other three sections, with one exception: the uppermost TN-16 lava from La Palma (Table 1).

The non-gaussian distribution of these lava ages reveals itself first by the excessive mean square of weighted deviates (MSWD) of 6.7 associated with the weighted mean age of 781.9 ± 1.5 kyr when all 23 isochrons in Table 1 are combined, and second, by the bimodal structure of the probability density distribution (Fig. 3). The older peak is defined by the three lowermost lavas at La Palma, plus the three Tahitian and nine Chilean ages, which are indistinguishable from one another and yield a weighted mean of 793.2 ± 2.5 kyr (MSWD = 0.7). In contrast, the weighted mean age of the six Haleakala lavas plus the TN-16 lava from La Palma is 775.5 ± 1.9 kyr (MSWD = 2.0); the difference between the younger and older groups of lavas is 17.7 ± 3.1 kyr.

Palaeointensity measurements from ODP site 983, where sedimentation rates of 13 cm kyr^{-1} maximize temporal resolution, show a prominent dip in intensity before the change in VGP and a concomitant drop in intensity that reflects the M–B reversal¹¹. The astronomical ages of the M–B reversal and the preceding dip in intensity determined at site 983 are 775 and 793 kyr, respectively¹¹. Evidently, this early dip in palaeointensity is a global feature of the magnetic field that, on the basis of astrochronological dating of a dozen Atlantic and Pacific cores^{10,24–25}, occurred ~ 15 kyr before the M–B reversal (Fig. 3).

The $^{40}\text{Ar}/^{39}\text{Ar}$ age of 776 ± 2 kyr for the Maui/upper La Palma lavas is identical to the astrochronological age of the M–B reversal of 778 ± 4 kyr globally²⁵, and 775 kyr at site 983 (ref. 11). Further, the older $^{40}\text{Ar}/^{39}\text{Ar}$ age of 793 ± 3 kyr for the lavas in Tahiti, Chile and

La Palma is identical to the astrochronological age of the precursor event both globally²⁵ and at ODP site 983 (ref. 11). Clement's finding¹³ that reversal duration is dependent on site latitude might suggest that even precise age determinations on transitionally magnetized lavas from distinct sites, each unable to continuously record field behaviour throughout a reversal, could result in spatial–temporal misinterpretation of the dynamo process. However, given both the synchronism between marine sediments^{11,25} and transitional lavas, and the proximity of Maui and Tahiti—hotspot islands only 38° apart (Fig. 2)—this is clearly not so in the present case. We therefore conclude that the transitional lavas from Tahiti, Chile and La Palma do not record the final directional reversal of the M–B transition, but instead provide a fragmentary snapshot of directions associated with the weakening of the field that preceded the reversal by 18 kyr.

We now argue that this extended period of unstable field behaviour may reflect the fact that the M–B was a successful polarity reversal. It has been suggested⁷ that the solid inner core largely controls the stability and hence the polarity of the dynamo field. Because the characteristic diffusion time for flux to escape the inner core is $\sim 10^3$ yr, it was suggested⁶ that the probability of a successful

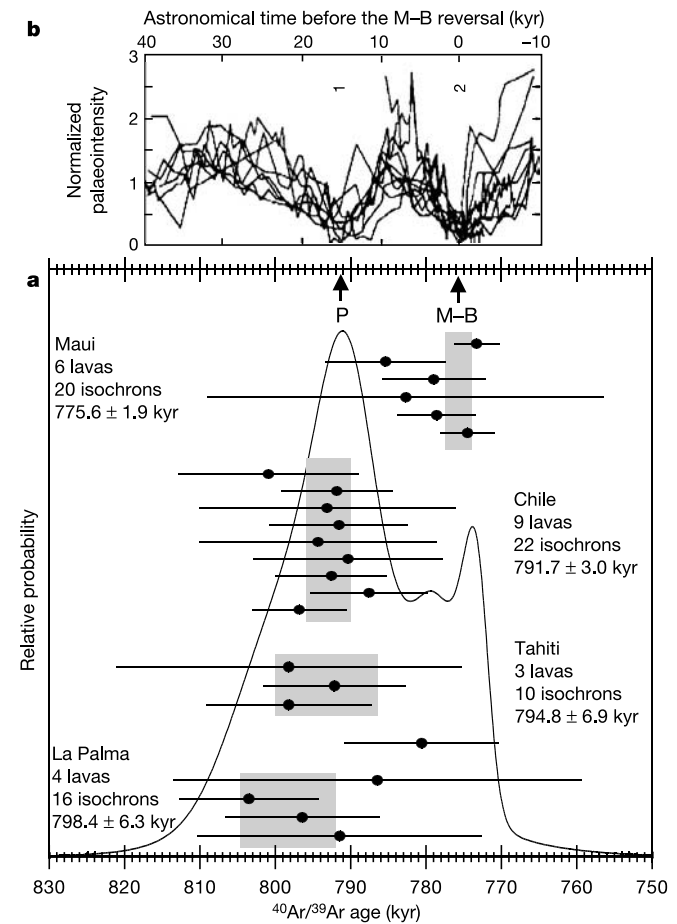


Figure 3 $^{40}\text{Ar}/^{39}\text{Ar}$ ages of 23 transitionally magnetized lava flows and palaeointensity records from 12 marine cores²⁵. **a**, Grey bands show the weighted mean age and 2σ uncertainty for each lava sequence. An exception is the uppermost lava from La Palma, which is younger than the underlying four lavas but coeval with lavas from Maui. The probability density curve indicates that these lavas span a minimum of 18 kyr. **b**, Normalized palaeointensity of sediments plotted so that the astronomical age of the M–B reversal matches the $^{40}\text{Ar}/^{39}\text{Ar}$ age of the Maui lavas (arrow at M–B). The precursory dip in intensity (arrow at P) is coeval with transitional lavas at Tahiti, La Palma and Chile.

reversal increases sharply as the duration of unstable outer-core field behaviour exceeds this value. The $^{40}\text{Ar}/^{39}\text{Ar}$ ages, indicating that dynamo instability lasted an order of magnitude longer than this diffusion time, offer the first radioisotopic observation supportive of this claim. It remains to be explored whether, to be successful, a reversal attempt requires an extended, multi-stage dynamo process like that seen not only for the M–B but also in other Cenozoic reversal records^{14,26}.

Examination of the modern-day non-axial dipole (NAD) field reveals that the global pattern of VGPs that would arise if the axial dipole field were to vanish is not random²⁷. In particular, a significant fraction of the Earth's surface encompassing the Pacific, including Tahiti, would experience field directions associated with south VGPs in and around Australia²⁷. Because the dynamo is blind to the sign of magnetic flux¹, the three most detailed records obtained from Tahitian lavas are wholly compatible with this simple model. Specifically, north VGPs associated with the R–R Punaruu^{15,20} and N–N Big Lost²⁷ events, as well as the N–R Jaramillo–Matuyama^{15,20} reversal, display a distinct preference for the Australasian region early in each record and contain a VGP cluster nearly identical to that of Tahitian M–B lavas shown in Fig. 3. Given the precise ages of the four M–B lava sequences, we can add another Tahitian result to this list. Along with the modern-day NAD-field analysis, these correspondences indicate that a mantle-controlled pattern of flux at the core surface might dominate the field configuration upon initiation of a dynamo instability when almost complete destruction of the axial dipole occurs. That transitional VGPs at this time on La Palma are found mainly elsewhere—over southern South America—lends support to a globally observed, largely non-dipolar early M–B field. Indeed, transitional M–B VGPs obtained from North Atlantic marine sediments^{9,28} indicate long-lived residences in this same locality.

Subsequent field behaviour associated with the actual polarity change might be more complex. Apparently, for the M–B transition, a significant fraction of the total 18 kyr of recorded instability elapsed before flux diffusion from the solid inner core allowed the reversal to proceed. □

Received 9 September 2004; accepted 31 January 2005; doi:10.1038/nature03431.

- Merrill, R. T. & McFadden, P. T. Geomagnetic polarity transitions. *Rev. Geophys.* **37**, 201–226 (1999).
- Laj, C., Mazaud, A., Weeks, R., Fuller, M. & Herrero-Bervera, E. Geomagnetic reversal paths. *Nature* **351**, 447 (1991).
- Glatzmaier, G. A., Coe, R. S., Hongre, L. & Roberts, P. H. The role of the Earth's mantle in controlling the frequency of geomagnetic reversals. *Nature* **401**, 885–890 (1999).
- Hoffman, K. A. Dipolar reversal states of the geomagnetic field and core-mantle dynamics. *Nature* **359**, 789–794 (1992).
- Coe, R. S. & Glen, J. M. G. The complexity of reversals. In *Timescales of the Paleomagnetic Field* (eds Channell, J. E. T., Kent, D. V., Lowrie, W. & Meert, J.) 221–232 (Am. Geophys. Un. Geophys. Monogr. 145, 2004).
- Gubbins, D. The distinction between geomagnetic excursions and reversals. *Geophys. J. Int.* **137**, F1–F3 (1999).
- Hollerbach, R. & Jones, C. A. Influence of the Earth's inner core on geomagnetic fluctuations and reversals. *Nature* **365**, 541–543 (1993).
- Laj, C., Guitton, S. & Kissel, C. Rapid changes and near-stationarity of the geomagnetic field during a polarity reversal. *Nature* **330**, 145–148 (1987).
- Channell, J. E. T. & Lehman, B. The last two geomagnetic polarity reversals recorded in high-deposition-rate sediment drifts. *Nature* **389**, 712–715 (1997).
- Kent, D. V. & Schneider, D. A. Correlation of paleointensity variation records in the Brunhes–Matuyama polarity transition interval. *Earth Planet. Sci. Lett.* **129**, 135–144 (1995).
- Channell, J. E. T. & Kleiven, H. F. Geomagnetic paleointensities and astrochronologic ages for the Matuyama–Brunhes boundary and the boundaries of the Jaramillo Subchron: paleomagnetic and oxygen isotope records from ODP site 983. *Phil. Trans. R. Soc. Lond. A* **358**, 1027–1047 (2000).
- Shackleton, N. J., Berger, A. & Peltier, W. R. An alternative astronomical calibration of the lower Pleistocene timescale based on ODP site 677. *Trans. R. Soc. Edinb. Earth Sci.* **81**, 251–261 (1990).
- Clement, B. Dependence of the duration of geomagnetic polarity reversal on site latitude. *Nature* **428**, 637–640 (2004).
- Hoffman, K. A. Transitional field behavior from southern hemisphere lavas: evidence for two-stage reversals of the geodynamo. *Nature* **320**, 228–232 (1986).
- Singer, B. S., Hoffman, K. A., Chauvin, A., Coe, R. S. & Pringle, M. S. Dating transitionally magnetized lavas of the late Matuyama Chron: Toward a new $^{40}\text{Ar}/^{39}\text{Ar}$ timescale of reversals and events. *J. Geophys. Res.* **104**, 679–693 (1999).
- Singer, B. S. *et al.* Ar/Ar ages of transitionally magnetized lavas on La Palma, Canary Islands, and the

- Geomagnetic Instability Timescale. *J. Geophys. Res. Solid Earth* **107**(B11), doi:10.1029/2001JB001613 (2002).
- Coe, R. S., Singer, B. S., Pringle, M. S. & Zhao, X. Matuyama–Brunhes reversal and Kamikatsura event on Maui: paleomagnetic directions, $^{40}\text{Ar}/^{39}\text{Ar}$ ages and implications. *Earth Planet. Sci. Lett.* **222**, 667–684 (2004).
- Brown, L., Singer, B. S., Pickens, J. & Jicha, B. Paleomagnetic directions and $^{40}\text{Ar}/^{39}\text{Ar}$ ages from the Tatara–San Pedro volcanic complex, Chilean Andes: Lava record of a Matuyama–Brunhes precursor? *J. Geophys. Res. Solid Earth* **109**(B12), doi:10.1029/2004JB003007 (2004).
- Love, J. J. & Mazaud, A. A database for the Matuyama–Brunhes magnetic reversal. *Phys. Earth Planet. Inter.* **103**, 207–245 (1997).
- Chauvin, A., Roperch, P. & Duncan, R. A. Records of geomagnetic reversals from volcanic islands of French Polynesia 2. Paleomagnetic study of a flow sequence (1.2 to 0.6 Ma) from the Island of Tahiti and discussion of reversal models. *J. Geophys. Res.* **95**, 2727–2752 (1990).
- Singer, B. S. & Pringle, M. S. Age and duration of the Matuyama–Brunhes geomagnetic polarity transition from $^{40}\text{Ar}/^{39}\text{Ar}$ incremental heating analyses of lavas. *Earth Planet. Sci. Lett.* **139**, 47–61 (1996).
- Brown, L., Pickens, J. & Singer, B. Matuyama–Brunhes transition recorded in lava flows of the Chilean Andes: Evidence for dipolar fields during reversals. *Geology* **22**, 299–302 (1994).
- Renne, P. R. *et al.* Intercalibration of standards, absolute ages and uncertainties in $^{40}\text{Ar}/^{39}\text{Ar}$ dating. *Chem. Geol.* **145**, 117–152 (1998).
- Tauxe, L., Herbert, T., Shackleton, N. J. & Kok, Y. S. Astronomical calibration of the Matuyama–Brunhes boundary: Consequences for magnetic remanence acquisition in marine carbonates and the Asian loess sequences. *Earth Planet. Sci. Lett.* **140**, 133–146 (1996).
- Hartl, P. & Tauxe, L. A precursor to the Matuyama/Brunhes transition-field instability as recorded in pelagic sediments. *Earth Planet. Sci. Lett.* **138**, 121–135 (1996).
- Prévot, M., Mankinen, E. A., Gromme, C. S. & Coe, R. S. How the geomagnetic field vector reverses polarity. *Nature* **316**, 230–234 (1985).
- Hoffman, K. A. & Singer, B. S. Regionally recurrent paleomagnetic transitional fields and mantle processes. In *Timescales of the Paleomagnetic Field* (eds Channell, J. E. T., Kent, D. V., Lowrie, W. & Meert, J.) 223–243 (Am. Geophys. Un. Geophys. Monogr. 145, 2004).
- Clement, B. M. & Kent, D. V. Geomagnetic polarity transition records from five hydraulic piston cores sites in the North Atlantic. In *Init. Rep. Deep Sea Drilling Project* (eds Ruddiman, W. F. *et al.*) **94**, 831–852 (US Government Printing Office, Washington, 1987).

Supplementary Information accompanies the paper on www.nature.com/nature.

Acknowledgements We thank J. Pickens, M. Relle, A. Battle, L. Powell and R. Allen for assistance with field work, argon and palaeomagnetic analyses, and graphics. This study was supported by the US NSF.

Competing interests statement The authors declare that they have no competing financial interests.

Correspondence and requests for materials should be addressed to B.S. (bsinger@geology.wisc.edu).

Sex increases the efficacy of natural selection in experimental yeast populations

Matthew R. Goddard*, H. Charles J. Godfray & Austin Burt

NERC Centre for Population Biology and Department of Biological Sciences, Imperial College London, Silwood Park Campus, Ascot SL5 7PY, UK

* Present address: School of Biological Sciences, The University of Auckland, Private Bag 92019, Auckland, New Zealand

Why sex evolved and persists is a problem for evolutionary biology, because sex disrupts favourable gene combinations and requires an expenditure of time and energy¹. Further, in organisms with unequal-sized gametes, the female transmits her genes at only half the rate of an asexual equivalent (the twofold cost of sex)². Many modern theories that provide an explanation for the advantage of sex incorporate an idea originally proposed by Weismann more than 100 years ago: sex allows natural selection to proceed more effectively because it increases genetic variation^{3–5}. Here we test this hypothesis, which still lacks robust empirical support, with the use of experiments on yeast populations. Capitalizing on recent advances in the molecular biology of recombination in yeast, we produced by genetic manipulation